

RESEARCH ARTICLE

Differential protein expression in heart in UT-B null mice with cardiac conduction defects

Hao Yu^{1*}, Yan Meng^{1*}, Li-Shun Wang^{2**}, Xian Jin², Li-Fang Gao¹, Lei Zhou¹, Kun Ji¹, Yang Li¹, Li-Juan Zhao¹, Guo-Qiang Chen², Xue-Jian Zhao¹ and Baoxue Yang^{3**}

¹ Department of Pathophysiology, Research Center of Prostate Diseases, School of Basic Medicine, Jilin University, Changchun, P. R. China

² Department of Pathophysiology, Ruijin Hospital, Shanghai Jiaotong University School of Medicine, Shanghai, P. R. China

³ Department of Pharmacology, School of Basic Medical Sciences, Peking University, Beijing, P. R. China

Cardiac conduction defects were found in transgenic mice deficient in urea transporter UT-B. To investigate the molecular mechanisms of the conduction defects caused by UT-B deletion, we studied the protein expression profiles of heart tissue (comprising most conduction system) in wild-type *versus* UT-B null mice at different ages. By two-dimensional electrophoresis-based comparative analysis, we found that more than dozen proteins were modulated (>two-fold) in the myocardium of UT-B null mice. Out of these modulated proteins, troponin T (TNNT2) presented significant changes in UT-B null mice at early stage prior to the development of P-R interval elongation, while the change of atrial natriuretic peptide (ANP) occurred only at late stage in UT-B null mice that had the AV block. These data indicate that UT-B deletion caused the dynamic expression regulation of TNNT2 and ANP, and these proteins may provide new clues to investigate the molecular events involved in cardiac conduction.

Received: 21 November, 2007

Revised: 7 July, 2008

Accepted: 19 August, 2008

Keywords:

Cardiac conduction block / Differential protein expression / Urea transporter / UT-B

1 Introduction

Cardiac conduction disease is a serious disorder of the heart. In the last decade the genes responsible for several inherited cardiac conduction diseases have been identified. If cardiac conduction disease is of an inherited nature, its underlying mechanisms can be either structural, functional, or overlap of these two mechanisms. Mutations in NK2 transcription

factor related, locus 5 (NKX2-5), protein kinase, AMP-activated, γ 2 noncatalytic subunit (PRKAG2), Lamin A/C (LMNA), and sodium channel, voltage-gated, type V, α (SCN5A) were found being involved in the first mechanism. Mutations in SCN5A, gap junction protein, fatty acid oxidation disorders, PRKAG2, and LMNA were found being involved in the second mechanism [1–9].

Urea transporters (UT) are a family of small integral membrane proteins that are specifically permeable to urea. The urea transporters cloned to date belong to two related subfamilies, the renal tubular-type UT-A and the erythrocyte-vascular type UT-B. UT-B is expressed in vasa recta descend-

Correspondence: Professor Xue-Jian Zhao, No. 8 Xinmin Road, Changchun, Jilin 130021, P. R. China

E-mail: pro_2@jlu.edu.cn

Fax: +86-431-85632348

Abbreviations: ANP, atrial natriuretic peptide; APOA1, apolipoprotein A-I precursor; HCM, hypertrophic cardiomyopathy; KS6A3, S6 kinase alpha 3; TNNT2, troponin T; UT, urea transporter

* These authors contributed equally to this work.

** Additional corresponding authors: Dr. Li-Shun Wang, E-mail: jywangls@shsmu.edu.cn; Professor Baoxue Yang, E-mail: baoyue@bjmu.edu.cn

ing through the outer and inner renal medulla [10], as well as in erythrocytes, testis, brain, bone marrow, thymus, liver, heart, lung, colon, urinary pelvic epithelium, urinary bladder, and spleen [11]. Humans carrying UT-B mutations (blood group Jk^{-/-}) have been identified lacking functional UT-B that manifest significantly reduced RBC urea permeability and a mild urinary concentrating defect [12–14]. UT-B deletion in mice caused severe urine concentrating deficiency [15, 16] and early mature in male reproductive system [17]. Our previous study found that UT-B null mice had cardiac conduction defects at ages older than 16 wk by Surface electrocardiogram (ECG) recording. The data showed that the P-R interval was significantly delayed in UT-B null mice at 16 wk old and the second degree AV block appeared in the UT-B null mice at 52 wk old [18]. The molecular mechanism in which UT-B deletion causes cardiac conduction block in UT-B null mice was not clear.

The objective of this investigation was to explore the proteins that are involved in cardiac conduction block promoted by UT-B deletion. We studied the dynamic changes in protein expression in the UT-B null mouse hearts with the first degree AV block and the second degree AV block using two-dimensional electrophoresis/mass spectra (2-DE/MS) approaches. The protein expression profiles of the myocardium in UT-B null mice were analyzed in comparison with that in age-matched wild-type mice. It was found that troponin (TNNT2) and atrial natriuretic peptide (ANP) were significantly regulated in the UT-B null hearts with cardiac conduction block. The results revealed that these proteins might be involved in the progress of cardiac conduction defect.

2 Materials and methods

2.1 Animals and treatment

UT-B null mice were generated as prescribed previously [18]. Wild-type mice from the same litter were used as control. All mice were treated following the protocol that was approved by the local ethics committee of Basic Medical Sciences of Jilin University. The mice were divided into four groups including wild-type and UT-B null mice at 16 and 52 wk old, respectively. There were five mice in each group. The mice were housed in a standard experimental animal laboratory with 12:12 h light-dark schedule and room temperature at 22°C, with free access to food and water.

2.2 Tissue preparation and examination

At 16 or 52 wk of age, the mice were anesthetized with an intraperitoneal injection of 5% chloral hydrate (1 mL/100 g body weight). The hearts were harvested following thoracotomy and washed with perfusion buffer (10 mM Tris-HCl, 250 mM sucrose, pH 7.0, at 4 °C).

2.3 2-DE

The wall of left ventricle was pulverized and mixed with 1.5 mL of 10% TCA in cold (–20°C) acetone containing 20 mM DTT. The samples were kept at –20°C overnight to allow complete precipitation. The samples were centrifuged for 30 min at 15 000 × *g*, washed twice with 1.5 mL acetone containing 20 mM DTT. Then the pellet was homogenized in 10 volumes of lysis buffer containing 7 M urea, 2 M thiourea, 4% w/v CHAPS, 40 mM Tris (base), and 1% v/v protease inhibitor cocktail (Sigma–Aldrich, MO, USA), followed by centrifuging at 40 000 × *g* for 60 min at 4°C. The protein concentration in suspension was determined using the BioRad AC DC protein assay kit (BioRad, Hercules, CA, USA). The samples were separated by 2-DE. The 17 cm IPG strips with a nonlinear range of pH 3–10 (BioRad, pH ranges used for IEF separation of proteins) were rehydrated for 12 h with 300 µL of solution containing 8 M urea, 2% w/v CHAPS, 20 mM DTT, 0.2% v/v Bio-lyte 3–10, 0.002% bromophenol blue and 100 µg protein. Electrofocusing was carried out for 60 kV·h at 20°C following the manufactory's instruction (BioRad). Prior to the second dimension, the IPG strips were equilibrated for 30 min with 50 mM Tris-HCl, pH 8.8, 6 M urea, 30% glycerol, 2% SDS, reduced with 1% of DTT, and alkylated with 5% iodoacetamide. The electrophoresed strips were then sealed on the top of the second-dimensional gels (12% SDS-polyacrylamide gel) with 0.5% agarose. The vertical second-dimensional electrophoresis was performed at constant current for 30 min at 16 mA *per gel*, and then at 24 mA *per gel* until the dye front reached the gel bottom. The separated proteins were visualized by silver staining. The silver staining procedure was a modification of a method described previously [19]. Proteins were fixed in the gel using 40% methanol and 10% acetic acid for 60 min. Then the gels were incubated in the sensitizing solution (30% v/v methanol, 1.25% w/v sodium thio-sulfate, and 0.5 M sodium acetate). Silver nitrate staining solution (0.25% w/v silver nitrate) and the developer (2.5% w/v sodium carbonate and 0.04% v/v formaldehyde) were used to visualize the proteins. Staining was stopped with stop solution (1.46% w/v EDTA) when gel background turned yellowish-brown. Experiments above were repeated five times for each animal. The images of the stained gels were acquired with an image scanner (GS-800 calibrated densitometry, BioRad), and analyzed with PDQuest 7.2.0 2D image analysis software (BioRad). The densities of the spots were determined after normalization based on the total spot volumes on the gel. The protein spots from different gels were matched. The match rate for protein spots from three samples in the same group was 84%, indicating a good reproducibility in our test system. The protein spots with significant changes in densities (paired *t*-test, *p* < 0.05) in a consistent direction (increase or decrease) were considered to be different, and selected for further identification.

2.4 Tryptic digestion and peptide extraction

After washing three times with Milli-Q water, the selected protein spots were transferred into the ZipPlate micro-SPE Plate wells (Millipore, Billerica, USA). The proteins were digested following the manufacturer's instruction (Millipore). Briefly, the selected gel pieces were incubated in the silver destaining solution containing 30 mM potassium ferri-cyanide and 100 mM sodium thiosulfate (1:1) for 20 min at room temperature in dark. After washing twice with Milli-Q water, the gel pieces were washed successively by 25 mM ammonium bicarbonate/5% ACN, twice by 25 mM ammonium bicarbonate/50% ACN and 100% ACN. Then the proteins were digested overnight with 10 μ L of 10 ng/ μ L sequencing grade modified porcine trypsin (Promega, Madison, WI, USA) in 25 mM ammonium bicarbonate at 37°C. The peptide fragments were extracted with 0.2% TFA for 30 min, and bound onto C18 resin, and then eluted with 0.2% TFA. Finally, the peptide mixtures were recovered by a 20 μ L elution solution containing 50% ACN/0.1% TFA [20].

2.5 Mass spectrometry

The tryptic peptides were then lyophilized and suspended in 2 μ L matrix solution containing 10 mg/mL CHCA in 50% ACN and 0.1% TFA. An aliquot of 0.7 μ L sample was spotted onto the MALDI sample target plate. The peptide mass spectra were obtained with a MALDI-TOF/TOF mass spectrometer (4700 Proteomics Analyzer, Applied Biosystems, Foster City, CA, USA). Prior to real sample acquisition, six calibrated spots were used for signal and parameter optimization. The PMF was obtained in the mass range between 800 and 4000 Da with *ca.* 3000 laser shots. To obtain the spectra with the mass accuracy less than 25 ppm, trypsin autolysis peaks were used for the internal calibration. Up to five most intense peaks, excluding those from the matrix, the background peaks, trypsin autolysis, acrylamide, or keratin peaks, were selected for subsequent MS/MS data acquisition. The collision gas pressure was adjusted to 5×10^{-7} Torr for MS/MS spectra acquisition.

2.6 Protein identification using database search algorithm

The proteins of interest were analyzed and identified by searching the Swiss-Prot protein database using the MASCOT search engine (Matrix Science) that was integrated into the Global Protein Server Workstation. For searching in the Rattus database and the Mus Musculus database, the mass tolerance (the most important parameter) was limited to 50 ppm. A maximum of one missed cleavages were allowed, and carbamidomethyl as well as oxidation of methionine were included. The results from both the MS and MS/MS spectra were accepted as a positive identification when the score confidence was higher than 95% by the Global Protein Server Workstation.

2.7 Western blot analysis

A total of 30 μ g protein mixed with SDS-PAGE buffer was loaded on 12% SDS-polyacrylamide gel for electrophoresis with the method described previously in detail [21]. The separated proteins were then transferred to nitrocellulose membranes (Axygen, CA, USA). The membrane was first incubated with blocking buffer containing 5% defatted milk powder, and then exposed to 0.1 μ g/mL mouse anti-human Troponin T (TNNT2) (Abcam, Cambridge, MA, USA) and rabbit antimouse ANP antibody (Chemicon, Temecula, CA, USA) for 2 h. The samples were then washed thoroughly with TBS buffer, followed by incubation with HRP-labeled antirabbit IgG secondary antibodies (1:2000, Abcam, Cambridge, MA, USA). The membranes were then washed, and examined for antigen-antibody complexes with diaminobenzidine and H₂O₂ (Santa Cruz, CA, USA). β -Actin was used as the internal control.

2.8 Statistical analysis

The data were expressed as mean \pm SD, and analyzed with the Student's *t*-test between two groups. It was considered statistically significant if *p*-value was less than 0.05.

3 Results and discussion

3.1 Altered protein expressions in UT-B null hearts with the early cardiac conduction block

Our previous study showed that the UT-B null mice had abnormal electrocardiogram compared to wild-type mice [18]. In UT-B null mice, the abnormal electrocardiogram appeared at 16 wk old and progressed at older age. Electrocardiogram showed P-R interval prolongation in UT-B null mice compared to wild-type mice at 52 wk old. About 20% UT-B mice had the second degree cardiac conduction block at 52 wk old. To study the mechanism in which the cardiac conduction block happened in UT-B null mice. The myocardial proteins of UT-B null mice and wild-type mice at 16 wk old were isolated and separated by 2-DE for comparative proteomic analysis. Totally 1245 ± 107 spots could be well separated according to image-analysis with PDQuest software. With the comparison of 2-DE images between UT-B null mice and wild-type mice, ten spots were found being significantly modulated in all three UT-B null mice (Fig. 1, Table 1). MALDI-TOF/TOF MS with PMF and MS/MS in combination with database searching showed that nine proteins were upregulated and one protein was downregulated. The proteins modulated in their expressions in UT-B null mice at 16 wk old can be sorted to four classes including proteins involved in cardiac muscle function (spots 8 and 14), cellular energy metabolism (spots 7, 15, and 17), ion channel function (spots 4, 6, 18, and 19), and oxidative stress (spot 16).

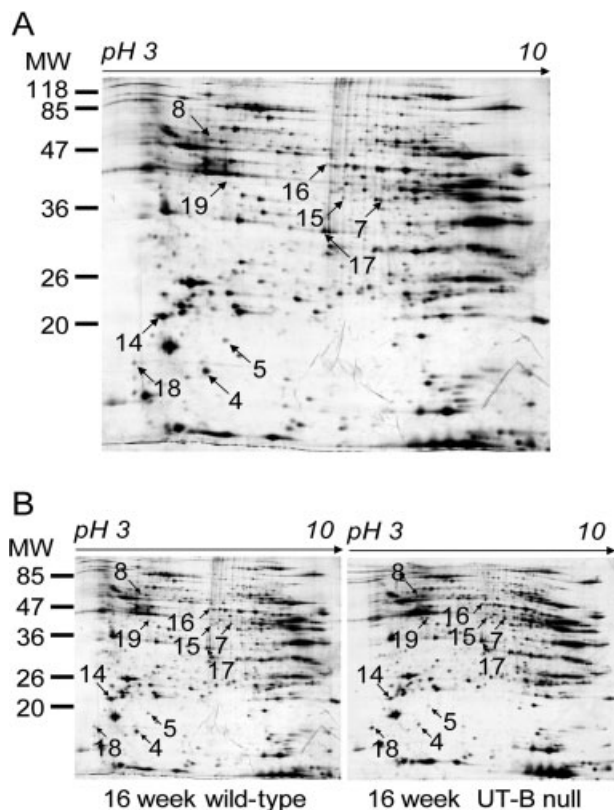


Figure 1. Identification of myocardial proteins and differentially expressed protein spots by 2-DE and MALDI-TOF MS in wild-type and UT-B null mice at 16 wk old. (A) A representative 2-DE map of myocardial proteins in 16 wk old wild-type mice. The spots with altered expression in UT-B null mice are marked with arrows. MW, molecular weight. (B) A pair of 2-DE maps of myocardial proteins from wild-type mice (left) and UT-B null mice (right) aged 16 wk.

The expression of myosin regulatory light chain 2 (MLRA) (spot 14) and desmin (spot 8), proteins involved in cardiac muscle function, were identified being altered in this study. These proteins play an important role in hypertrophic cardiomyopathy (HCM) and other cardiac diseases [22]. The expression of acyl-CoA (spots 7 and 15), an important enzyme for fatty acid oxidation [23], was dramatically upregulated. The expression of malate dehydrogenase cytoplasmic (spot 17), a key enzyme of mitochondrial oxidant phosphorylation [24], was dramatically upregulated. These results indicated a decreased glycolysis and increased oxidation of fatty acid and glucose may promote heart conduction block in UT-B null mice. Interestingly, α -enolase (spot 16), a key enzyme for glucose oxidation related to energy metabolism, was found being upregulated in the present study. These modulations happened in UT-B null mice at 16 wk old. Eukaryotic translation initiation factor 5A (spot 4), a monomeric protein, in conjunction with GTP and other initiation factors plays an essential role in the initiation of protein synthesis in eukaryotic cells [25]. The increased expression of ion channel protein, troponin I, troponin C, and TNNT2 were significantly upregulated in UT-B null mice.

3.2 Altered expression of proteins S6 kinase alpha 3 (KS6A3), apolipoprotein A-I precursor (APOA1), ANP, and TNNT2 in the hearts with conduction block in UT-B null mice at 52 wk old

As found in previous studies [18], the cardiac conduction block in UT-B null mice is even severer at 52 wk old than that in UT-B null mice at 16 wk old. We speculated that some specific proteins would be involved in cardiac conduction block in UT-B mice at old ages. Thus, the protein expression profiles of the heart were compared between UT-B null mice and wild-type mice at age of 52 wk (Fig. 2). The results showed that expression levels of four proteins (KS6A3, APOA1, ANP, and TNNT2) were significantly changed in UT-B null mice, of which one could also be revealed at 16 wk old, and three were only identified at 52 wk old (Fig. 3 and Table 2). Two of them were downregulated including ribosomal protein KS6A3 (spot 1), two proteins were upregulated including APOA1 (spot 7), and ANP (spot 10). Interestingly,

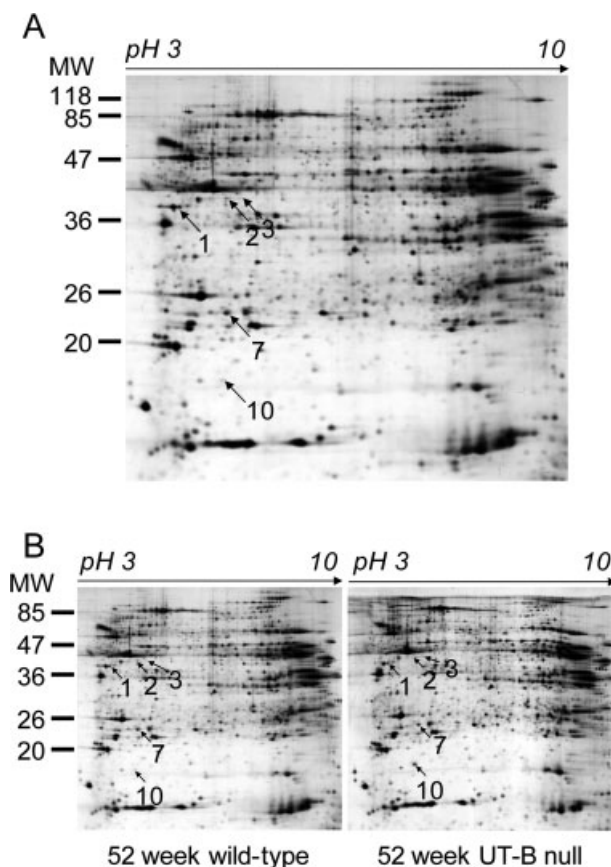


Figure 2. Identification of myocardial proteins and differentially expressed protein spots by 2-DE and MALDI-TOF MS in 52 wk old wild-type and UT-B null mice. (A) A representative 2-DE map of myocardial proteins in 52 wk old wild-type mice. The spots with altered expression in UT-B null mice are marked with arrows in the map. MW, molecular weight. (B) A pair of 2-DE maps of myocardial proteins from wild-type mice (left) and UT-B null mice (right) aged 52 wk.

Table 1. Identified altered proteins in heart of 16 wk UT-B knock-out mouse

Classification/ gene symbol	Protein name	Acc. no.	Spot no.	Mean-fold N/C (<i>n</i> = 5) UT-B knock out/wild-type	<i>p</i> / (theor./ exptl.)	MW (theor./ exptl.)	PMF			MS/MS	
							Pep.	Cov.	Sco.	Pep.	Sco.
Resident protein in mitochondria											
IF5A	Eukaryotic translation initiation factor 5A	P63242	K4	2.479 ± 0.33	5.08	16 918	5	43	46	1	24
TNNI3	Troponin I, cardiac muscle	P48787	K6	2.163 ± 0.31	9.57	24 227	11	40	48		
ACADS	Acyl-CoA dehydrogenase, short-chain specific mitochondrial precursor	Q07417	K7	5.127 ± 0.29	8.96	45 203	23	45	157	2	80
DESM	Desmin	P31001	K8	2.822 ± 0.37	5.21	53 391	39	68	305		
MLRA	Myosin regulatory light chain 2	Q9QVP4	K14	−2.211 ± 0.31	4.76	19 609	16	74	131		
ACADS	Acyl-CoA dehydrogenase, short-chain specific mitochondrial precursor	Q07417	K15	2.123 ± 0.14	8.96	45 203	12	33	77	2	81
ENOA	α-Enolase (2-phospho-D- glycerate hydro-lyase)	P17182	K16	2.202 ± 0.10	6.36	47 322	11	34	73		
MDHC	Malate dehydrogenase, cytoplasmic	P14152	K17	2.293 ± 0.15	6.16	36 494	10	35	66		
TNNC1	Troponin C, slow skeletal and cardiac muscle(TN-C)	P19123	K18	6.033 ± 0.47	4.04	18 523	12	63	78	3	178
TNNT2	Troponin T, cardiac muscle (tntc)	P50752	K19	5.614 ± 0.40	4.98	35 673	15	36	119	3	99

Table 2. Identified altered proteins in heart of 16 and 52 weeks UT-B knock-out mouse

Classification/ gene symbol	Protein name	Acc. no.	Spot no.	Mean-fold N/C (<i>n</i> = 5) 52 wk/16 wk	<i>p</i> / (theor./ exptl.)	MW (theor./ exptl.)	PMF			MS/MS	
							Pep.	Cov.	Sco.	Pep.	Sco.
Resident protein in mitochondria											
KS6A3	Ribosomal protein S6 kinase α3	P18654	K1	−2.012 ± 0.16	6.41	83 983	12	20	60		
TNNT2	Troponin T, cardiac muscle (TnTc)	P50752	K2	−3.970 ± 0.20	4.98	35 673	13	27	103	2	26
TNNT2	Troponin T, cardiac muscle (TnTc)	P50752	K3	−4.000 ± 0.39	4.98	35 673	13	27	103	2	26
APOA1	Apolipoprotein A-I precursor	Q00623	K7	4.124 ± 0.56	5.64	30 569	16	40	103	2	57
ANP	Atrial natriuretic peptide	P05125	K10	4.039 ± 0.59	6.73	16 748	5	25	38	3	134

TNNT2 is only protein which expression level was changed in both 16 and 52 wk old UT-B mice. But it (spot 19) was upregulated in 16 wk old UT-B mice and downregulated (spots 2 and 3) in 52 wk old UT-B mice. The data indicate that TNNT2 may play an important role in the development of cardiac conduction defects. The mechanism in which TNNT2 is involved in cardiac conduction block remains to be studied.

3.3 The dynamic expression of ANP in heart of UT-B null mice

Natriuretic peptides are a group of naturally occurring substances that act in the body to oppose the activity of the renin-

angiotensin system. ANP is synthesized in the atria [26]. The expression level of ANP was similar in the 16 and 52 wk old wild-type mice. Interestingly, the ANP was significantly upregulated in 52 wk old UT-B null mice (with the second degree cardiac conduction block) compared to 16 wk old UT-B null mice (with the first degree cardiac conduction block) and 52 wk old wild-type mice (without cardiac conduction block), which indicates that changes in this protein expression pattern might be associated with late cardiac conduction block (Fig. 4).

Previous studies showed that the dramatic increase in ANP release produced by cardiac ischemia appears to be mediated in part by endothelin [27]. Nitric oxide (NO), an

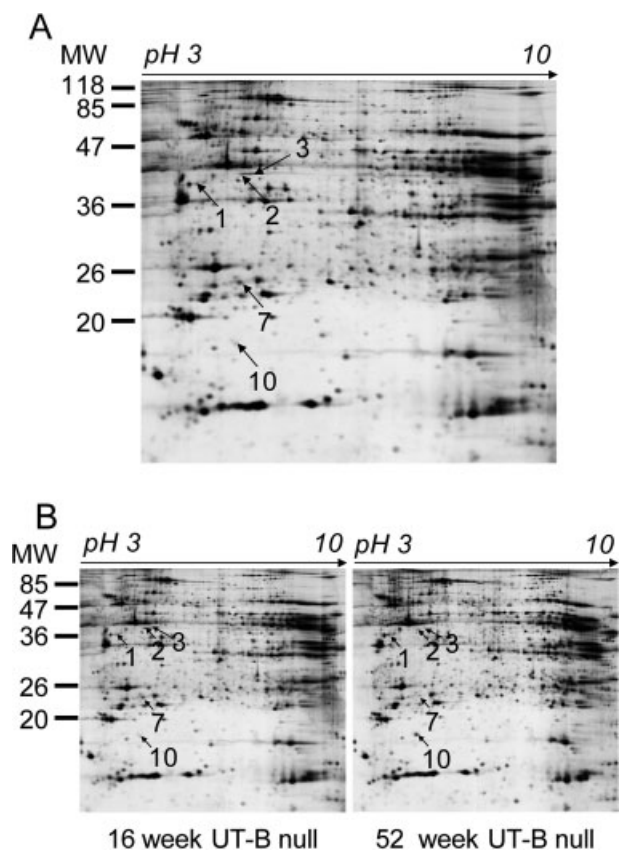


Figure 3. Identification of myocardial proteins and differentially expressed protein spots by 2-DE and MALDI-TOF MS in 16 and 52 wk old UT-B null mice. (A) A representative 2-DE map of myocardial proteins in 16 wk old UT-B null mice. MW, molecular weight. (B) A pair of 2-DE maps of myocardial proteins in 16 wk old UT-B null mice (left) and 52 wk old UT-B null mice (right). The spots with altered expression are marked with arrows.

important vasodilator, is also produced by endothelial cells and inhibits ANP secretion acting through cyclic GMP as an intracellular messenger. Several recent studies have defined the cellular mechanism contributing to the regulation of ANP secretion including stretch-activated ion channels, prostaglandins, cytochrome P450, G proteins, and cell calcium [27]. A number of steps in the cellular ANP signal transduction remain to be determined. The release of ANP in disease states such as myocardial infarction and heart failure appears to be related to both mechanical and cellular events [27, 28]. ANP had been thought to be the gold standard of cardiac hypertrophy [29–31]. Almost all familial heart block had the character of cardiac hypertrophy [32]. Therefore, the modulations of ANP in UT-B null mice hint that cardiac hypertrophy may be involved in the mechanism of heart block in mice.

Natriuretic peptide system consists of three endogenous ligands, ANP, brain natriuretic peptide (BNP), and C-type natriuretic peptide (CNP). They contribute to the regulation of cardiovascular homeostasis through diuretic, natriuretic,

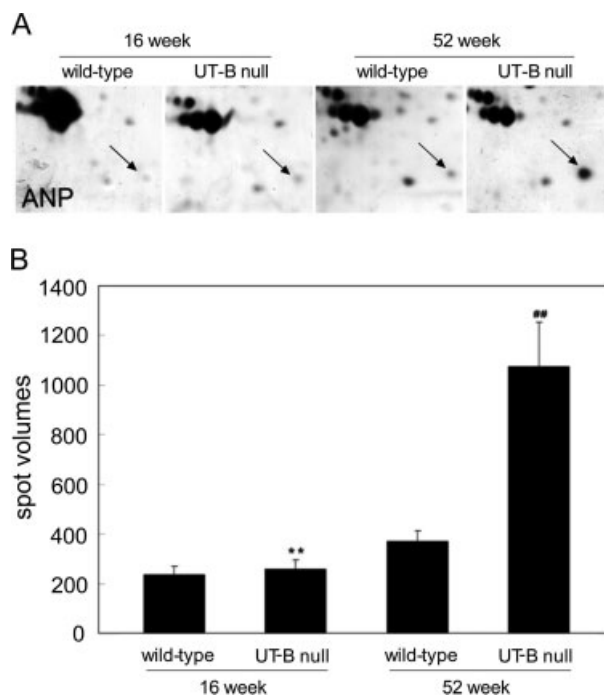


Figure 4. The expression level of ANP in 16 and 52 wk old UT-B null mice. (A) The density of spot 10 in Fig. 3 (identified as ANP in Table 2) is indicated with arrow. (B) The bar graph shows the relative spot densities. ** $p < 0.01$ versus wild-type mice at 16 wk old, ## $p < 0.01$ versus wild-type mice at 52 wk old.

and vasodilatory properties. ANP has drawn particular attention because of its effects on blood pressure regulation and cardiac function. Recently, ANP has also been regarded as a possible cardiovascular risk factor [33]. BNP has emerged as a relevant marker of left ventricular (LV) dysfunction and as a useful predictor of the outcome in patients with heart failure. CNP can modulate the phenotype of vascular smooth muscle cells to regulate vascular remodeling [34]. Maybe the ANP might modulate myocardial cells to regulate myocardial remodeling. We conjecture that myocardial remodeling lead to the up-regulation of ANP expression in the 52 wk old UT-B null mice. The myocardial remodeling may be another reason of cardiac conduction defect in 52 wk old UT-B null mice.

3.4 The dynamic expression of TNNT2 in UT-B null mice

The contraction of striated muscle is regulated by troponin (Tn) complex, which acts as a Ca^{2+} sensor [35]. TNNT2 is a subunit of cardiac troponin that plays an important role in many heart diseases and renal diseases. Intriguingly, the expression of TNNT2 was found to be significantly upregulated in 16 wk old UT-B null mice compared to the same aged wild-type mice. The expression of TNNT2 in 52 wk old UT-B null mice was as the same level as that in 16 wk old

wild-type mice. The expression of TNNT2 was compensatively increased in 16 wk old UT-B null mice. The findings were also confirmed by Western blot analysis (Figs. 5 and 6).

Series of studies showed that the gene mutation of TNNT2 is a direct cause of the familial HCM (FHC), dilated cardiomyopathy (DCM), and other heart disease [35]. The cardiac troponin C_{TnT} as well as tropomyosin has been associated with HCM. However, C_{TnT} accounts for most of the mutations that cause HCM in these regulatory proteins. To date 30 mutations have been identified in the cardiac C_{TnT} gene that results in familial HCM (FHC) [36]. Over the last 10 years, several reports about the physiological roles of these isoforms in human heart have been presented.

QT dispersion is a sign to evaluate if human have cardiac arrhythmia or not. The QT dispersion is positive correlation with myocardial damage. The C_{TnT} was used as a biomarker of myocardial damage [37]. The C_{TnT} was significantly higher in UT-B null mice than that in wild-type mice at 16 wk old, which indicates that reversible myocardial damage leads to cardiac conduction block in UT-B null mice.

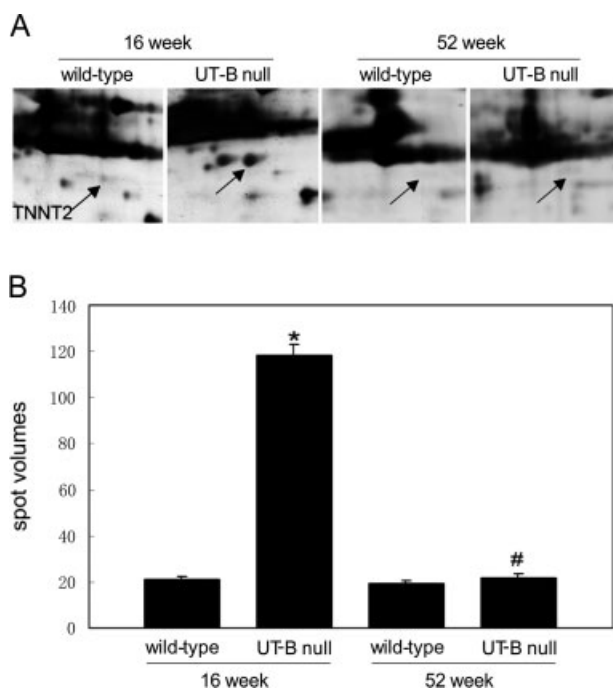


Figure 5. The expression level of TNNT2 in 16 wk-old wild-type and UT-B null mice. (A) Spot volume of spot 19 in Fig. 1 (identified as TNNT2 in Table 1) is indicated with arrow. (B) The bar graph shows the relative spot densities. * $p < 0.01$ versus wild-type mice at 16 wk old, # $p < 0.01$ versus wild-type at 52 wk old.

4 Conclusions

In summary, the expression levels of some proteins involved in cellular energy metabolism and ion channel proteins were significantly modified before and after the development of

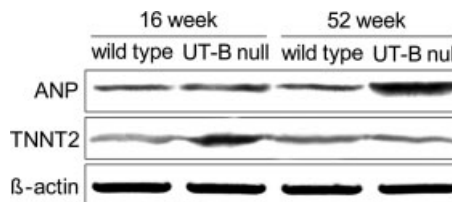


Figure 6. Western blot analysis of the expression levels of ANP and TNNT2 in 16 and 52 wk old wild-type and UT-B null mice. β -Actin is used as reference control.

cardiac conduction block in UT-B null mice. The results revealed that these proteins might be involved in the progress of cardiac conduction defect. However, further investigations remain to be performed to study the basic pathophysiological mechanisms in which cardiac conduction block occurs in UT-B null mice.

This work was supported by National Natural Science Foundation of China grant 30370572 (X.-J. Z), Ministry of Science and Technology grant 2006AA02Z105 (L.-S. W.), National Natural Science Foundation of China grant 30870921, and 985 Projects of Ministry of Education of China (B. Y.).

The authors have declared no conflict of interest.

5 References

- [1] Gollob, M. H., Green, M. S., Tang, A. S., Gollob, T. *et al.*, Identification of a gene responsible for familial Wolff-Parkinson-White syndrome. *New Engl. J. Med.* 2001, **344**, 1823–1831.
- [2] Gollob, M. H., Seger, J. J., Gollob, T. N., Tapscott, T. *et al.*, Novel PRKAG2 mutation responsible for the genetic syndrome of ventricular preexcitation and conduction system disease with childhood onset and absence of cardiac hypertrophy. *Circulation* 2001, **104**, 3030–3033.
- [3] Saudubray, J. M., Martin, D., de Lonlay, P., Touati, G. *et al.*, Recognition and management of fatty acid oxidation defects: a series of 107 patients. *J. Inherit. Metab. Dis.* 1999, **22**, 488–502.
- [4] Ou, Y., Strege, P., Miller, S. M., Makielski, J. *et al.*, Syntrophin gamma 2 regulates SCN5A gating by a PDZ domain-mediated interaction. *J. Biol. Chem.* 2003, **278**, 1915–1923.
- [5] Smits, J. P., Koopmann, T. T., Wilders, R., Veldkamp, M. W. *et al.*, A mutation in the human cardiac sodium channel (E161K) contributes to sick sinus syndrome, conduction disease and Brugada syndrome in two families. *J. Mol. Cell. Cardiol.* 2005, **38**, 969–981.
- [6] Tawil, R., Ptacek, L. J., Pavlakis, S. G., DeVivo, D. C. *et al.*, Andersen's syndrome: Potassium-sensitive periodic paralysis, ventricular ectopy, and dysmorphic features. *Ann. Neurol.* 1994, **35**, 326–330.
- [7] Lahat, H., Pras, E., Olender, T., Avidan, N. *et al.*, A missense mutation in a highly conserved region of CASQ2 is associated with autosomal recessive catecholamine-induced poly-

- morphic ventricular tachycardia in Bedouin families from Israel. *Am. J. Hum. Genet.* 2001, *69*, 1378–1384.
- [8] Thomas, S. A., Schuessler, R. B., Berul, C. I., Beardslee, M. A. *et al.*, Disparate effects of deficient expression of connexin43 on atrial and ventricular conduction: Evidence for chamber-specific molecular determinants of conduction. *Circulation* 1998, *97*, 686–691.
- [9] Liu, M. R., Pan, K. F., Li, Z. F., Wang, Y. *et al.*, Rapid screening mitochondrial DNA mutation by using denaturing high-performance liquid chromatography. *World J. Gastroenterol.* 2002, *8*, 426–430.
- [10] Timmer, R. T., Klein, J. D., Bagnasco, S. M., Doran, J. J. *et al.*, Localization of the urea transporter UT-B protein in human and rat erythrocytes and tissues. *Am. J. Physiol.* 2001, *281*, C1318–C1325.
- [11] Yang, B., Bankir, L., Urea and urine concentrating ability: New insights from studies in mice. *Am. J. Physiol. Renal. Physiol.* 2005, *288*, F881–F896.
- [12] Lucien, N., Sidoux-Walter, F., Olives, B., Moulds, J. *et al.*, Characterization of the gene encoding the human Kidd blood group/urea transporter protein. Evidence for splice site mutations in Jknull individuals. *J. Biol. Chem.* 1998, *273*, 12973–12980.
- [13] Sands, J. M., Gargus, J. J., Frohlich, O., Gunn, R. B., Kokko, J. P., Urinary concentrating ability in patients with Jk(a-b-) blood type who lack carrier-mediated urea transport. *J. Am. Soc. Nephrol.* 1992, *2*, 1689–1696.
- [14] Meng, Y., Zhou, X., Li, Y., Zhao, D. *et al.*, A novel mutation at the JK locus causing Jk null phenotype in a Chinese family. *Sci. China, C, Life Sci.* 2005, *48*, 636–640.
- [15] Yang, B., Verkman, A. S., Analysis of double knockout mice lacking aquaporin-1 and urea transporter UT-B. Evidence for UT-B-facilitated water transport in erythrocytes. *J. Biol. Chem.* 2002, *277*, 36782–36786.
- [16] Bankir, L., Chen, K., Yang, B., Lack of UT-B in vasa recta and red blood cells prevents urea-induced improvement of urinary concentrating ability. *Am. J. Physiol.* 2004, *286*, F144–F151.
- [17] Guo, L., Zhao, D., Song, Y., Meng, Y. *et al.*, Reduced urea flux across the blood-testis barrier and early maturation in the male reproductive system in UT-B-null mice. *Am. J. Physiol.* 2007, *293*, C305–C312.
- [18] Meng, Y., Zhang, X. X., Zhao, H., Guo, L. *et al.*, The changes of ECG and action potential in mice lacking urea transporter. *Sci. China* 2007, *37*, 447–451.
- [19] Rabilloud, T., Brodard, V., Peltre, G., Righetti, P. G., Ettori, C., Modified silver staining for immobilized pH gradients. *Electrophoresis* 1992, *13*, 264–266.
- [20] Tu, L. C., Yan, X., Hood, L., Lin, B., Proteomics analysis of the interactome of N-myc downstream regulated gene 1 and its interactions with the androgen response program in prostate cancer cells. *Mol. Cell. Proteomics* 2007, *6*, 575–588.
- [21] Nakajima, K., Hamanoue, M., Takemoto, N., Hattori, T. *et al.*, Plasminogen binds specifically to alpha-enolase on rat neuronal plasma membrane. *J. Neurochem.* 1994, *63*, 2048–2057.
- [22] Blair, E., Redwood, C., de Jesus Oliveira, M., Moolman-Smoock, J. C. *et al.*, Mutations of the light meromyosin domain of the beta-myosin heavy chain rod in hypertrophic cardiomyopathy. *Cir. Res.* 2002, *90*, 263–269.
- [23] Newsholme, P., Keane, D., Welters, H. J., Morgan, N. G., Life and death decisions of the pancreatic beta-cell: The role of fatty acids. *Clin. Sci. (Lond.)* 2007, *112*, 27–42.
- [24] Burt, H. M., Jackson, J. K., Dryden, P., Salari, H., Crystal-induced protein tyrosine phosphorylation in neutrophils and the effect of a tyrosine kinase inhibitor on neutrophil responses. *Mol. Pharm.* 1993, *43*, 30–36.
- [25] Das, S., Maitra, U., Functional significance and mechanism of eIF5-promoted GTP hydrolysis in eukaryotic translation initiation. *Prog. Nucleic Acid Res. Mol. Biol.* 2001, *70*, 207–231.
- [26] Cho, Y., Somer, B. G., Amatya, A., Natriuretic peptides and their therapeutic potential. *Heart Dis.* 1999, *1*, 305–328.
- [27] Dietz, J. R., Mechanisms of atrial natriuretic peptide secretion from the atrium. *Cardiovasc. Res.* 2005, *68*, 8–17.
- [28] Woodard, G. E., Rosado, J. A., Brown, J., Expression and control of C-type natriuretic peptide in rat vascular smooth muscle cells. *Am. J. Physiol. Regul. Integr. Comp. Physiol.* 2002, *282*, R156–R165.
- [29] Iyengar, S., Haas, G., Lamba, S., Orsinelli, D. A. *et al.*, Effect of cardiac resynchronization therapy on myocardial gene expression in patients with nonischemic dilated cardiomyopathy. *J. Card. Fail.* 2007, *13*, 304–311.
- [30] Luchner, A., Brockel, U., Muscholl, M., Hense, H. W. *et al.*, Gender-specific differences of cardiac remodeling in subjects with left ventricular dysfunction: a population-based study. *Cardiovasc. Res.* 2002, *53*, 720–727.
- [31] Morawietz, H., Szibor, M., Goettsch, W., Bartling, B. *et al.*, Unloading of the left ventricle by ventricular assist device normalizes increased expression of endothelin ET(A) receptors but not endothelin-converting enzyme-1 in patients with end-stage heart failure. *Circulation* 2000, *102*, III188–III193.
- [32] Gietzen, F. H., Leuner, C. J., Obergassel, L., Strunk-Mueller, C., Kuhn, H., Transcatheter ablation of septal hypertrophy for hypertrophic obstructive cardiomyopathy: feasibility, clinical benefit, and short term results in elderly patients. *Heart* 2004, *90*, 638–644.
- [33] Rubattu, S. S. S., Valenti, V., Stanzione, R., Volpe, M., Natriuretic peptides: An update on bioactivity, potential therapeutic use, and implication in cardiovascular diseases. *Am. J. Hypertens.* 2008, *21*, 733–741.
- [34] Itoh, H., Nakao, K., Natriuretic peptide system. *Nippon Rinsho* 1997, *55*, 1923–1936.
- [35] Gomes, A. V., Potter, J. D., Molecular and cellular aspects of troponin cardiomyopathies. *Ann. N. Y. Acad. Sci.* 2004, *1015*, 214–224.
- [36] Gomes, A. V., Barnes, J. A., Harada, K., Potter, J. D., Role of troponin T in disease. *Mol. Cell. Biochem.* 2004, *263*, 115–129.
- [37] Adamcova, M., Sterba, M., Simunek, T., Potacova, A. *et al.*, Troponin as a marker of myocardial damage in drug-induced cardiotoxicity. *Exp. Opin. Drug Safety* 2005, *4*, 457–472.